

Quantitative neuropathology associated with chronic manganese exposure in South African mine workers

Luis F. Gonzalez-Cuyar^a, Gill Nelson^b, Susan R. Criswell^c, Pokuan Ho^d, Jaymes A. Lonzanida^d, Harvey Checkoway^{e,f}, Noah Seixas^e, Benjamin B. Gelman^{g,h,i}, Bradley A. Evanoff^j, Jill Murray^{b,k}, Jing Zhang^a, Brad A. Racette^{b,c,*}

^a Department of Pathology, Division of Neuropathology, University of Washington, School of Medicine, Seattle, WA, USA

^b School of Public Health, Faculty of Health Sciences, University of the Witwatersrand, Parktown, South Africa

^c Department of Neurology, Washington University School of Medicine, Saint Louis, MO, USA

^d Department of Biology, University of Washington, Seattle, WA, USA

^e Department of Environmental and Occupational Health, University of Washington, Seattle, WA, USA

^f Department of Family Medicine and Preventive Medicine, University of California, San Diego, La Jolla, CA, USA

^g Department of Pathology, University of Texas Medical Branch, Galveston, TX, USA

^h Department of Neuroscience, University of Texas Medical Branch, Galveston, TX, USA

ⁱ Department of Cell Biology, University of Texas Medical Branch, Galveston, TX, USA

^j Department of Medicine, Washington University School of Medicine, Saint Louis, MO, USA

^k National Institute for Occupational Health, National Health Laboratory Service, Johannesburg, South Africa

ARTICLE INFO

Article history:

Received 31 May 2013

Received in revised form 6 December 2013

Accepted 19 December 2013

Available online 26 December 2013

ABSTRACT

Manganese (Mn) is a common neurotoxicant associated with a clinical syndrome that includes signs and symptoms referable to the basal ganglia. Despite many advances in understanding the pathophysiology of Mn neurotoxicity in humans, with molecular and structural imaging techniques, only a few case reports describe the associated pathological findings, and all are in symptomatic subjects exposed to relatively high-level Mn. We performed an exploratory, neurohistopathological study to investigate the changes in the corpus striatum (caudate nucleus, putamen, and globus pallidus) associated with chronic low-level Mn exposure in South African Mn mine workers. Immunohistochemical techniques were used to quantify cell density of neuronal and glial components of the corpus striatum in eight South African Mn mine workers without clinical evidence of a movement disorder and eight age-race-gender matched, non-Mn mine workers. There was higher mean microglia density in Mn mine workers than non-Mn mine workers in the globus pallidus external and internal segments [GPe: 1.33 and 0.87 cells per HPF, respectively ($p = 0.064$); GPi: 1.37 and 0.99 cells per HPF, respectively ($p = 0.250$)]. The number of years worked in the Mn mines was significantly correlated with microglial density in the GPi (Spearman's rho 0.886; $p = 0.019$). The ratio of astrocytes to microglia in each brain region was lower in the Mn mine workers than the non-Mn mine workers in the caudate (7.80 and 14.68; $p = 0.025$), putamen (7.35 and 11.11; $p = 0.117$), GPe (10.60 and 16.10; $p = 0.091$) and GPi (9.56 and 12.42; $p = 0.376$). Future studies incorporating more detailed occupational exposures in a larger sample of Mn mine workers will be needed to demonstrate an etiologic relationship between Mn exposure and these pathological findings.

© 2014 Elsevier Inc. All rights reserved.

1. Introduction

Manganese (Mn), an essential trace element, physiologically acts as a cofactor for multiple enzymes, including pyruvate carboxylase and Mn superoxide dismutase (Bowman et al., 2011;

Milatovic et al., 2009; Sidoryk-Wegrzynowicz et al., 2009). When ingested, Mn is tightly regulated and excreted in the bile; however, when absorbed through the respiratory tract, this homeostatic regulation is bypassed (Teeguarden et al., 2007a, 2007b). The original reports of workers exposed to very high levels of Mn described workers with an atypical parkinsonian phenotype, including dystonia, early gait impairment, behavioral dysfunction, and cognitive impairment (Couper, 1837; Rodier, 1955; Wang et al., 1989). However, modern occupational exposures are an order of magnitude lower than these historical exposures, and the resulting clinical phenotype appears to be substantially different

* Corresponding author at: Department of Neurology, Washington University School of Medicine, 660 South Euclid Avenue, Campus Box 8111, Saint Louis, MO 63110, USA. Tel.: +1 314 747 0532; fax: +1 314 747 3258.

E-mail address: racetteb@neuro.wustl.edu (B.A. Racette).

(Rodier, 1955; Racette et al., 2012, 2005; Flynn and Susi, 2010; Cooper, 1984; Liu et al., 2011; Hobson et al., 2011). Clinical-pathological studies provide the most definitive pathophysiological data to explain the observed phenotypic differences between past and current exposures to Mn. However, these studies are very difficult to conduct due to limited access to neuropathology expertise, long periods between working in an occupation where Mn exposure occurs and time of death, and reluctance of families to pursue autopsies.

To the best of our knowledge, since the first clinical description of manganism in 1837, only eight gross neuropathological examinations have been reported in subjects with high occupational Mn exposures (Couper, 1837; Rodier, 1955; Ashizawa, 1927; Canavan et al., 1934; Casamajor, 1913; Stadler, 1936; Trendtel, 1936; Yamada et al., 1986). Seven of these were qualitative histopathological examinations without immunohistochemical preparations. A 1913 report described a symptomatic Mn separating-mill worker with normal gross neuropathology, but no histopathological examination was performed (Casamajor, 1913). From 1927 to 1954, four case studies were reported, having undergone qualitative histopathological examination: a symptomatic brownstone miller with neuronal loss in the globus pallidus and an intact substantia nigra; a symptomatic dock worker with neuronal loss and concomitant gliosis of the corpus striatum; a symptomatic brownstone miller with putaminal and pallidal neuronal loss and gliosis with preservation of the substantia nigra; and a symptomatic brownstone miller with significant neuronal death in the globus pallidus with a grossly well-pigmented substantia nigra (Ashizawa, 1927; Stadler, 1936; Parnitzke, 1954; Trendtel, 1936). In the only Mn neuropathology study that included a reference subject for comparison, a 55-year-old male mill worker with manganism demonstrated gross atrophy of the basal ganglia and compensatory ventriculomegaly compared to a 55-year-old woman who died of tuberculosis (Canavan et al., 1934). Histopathological comparison revealed greater density of glia and neurons in the caudate and lenticular nuclei in the mill worker. However, this study preceded the current availability of more precise immunohistochemical methods. Subsequently, post mortem gross examination of a 67-year-old woman exposed to manganese dioxide as a battery factory worker, who developed manganism, revealed atrophy of the pallidum as well as microscopic cortical, rubral, and striatal astrogliosis with spotty degeneration of the substantia nigra pars compacta and occasional nigral Lewy bodies (Bernheimer et al., 1973). The most recent histopathological report described a symptomatic Mn ore-crushing factory worker with gross atrophy and discoloration of the globus pallidus as well as histopathological evidence of neuronal loss, a moderate increase in astrocytes in the corpus striatum, and normal substantia nigra (Yamada et al., 1986).

Despite recognition of an Mn neurotoxicity syndrome for nearly 200 years, very few post mortem neuropathological studies in humans with documented Mn exposures have been reported in the literature. These reports comprise qualitative post-mortem histopathological evaluations which lack quantitative data, with the exception of one case report, or immunohistochemical/immunofluorescent evaluations. While these reports provide some insight into the neuropathological effects of Mn exposure, they ultimately describe the end-stage changes of the Mn neurotoxicity syndrome that is rarely, if ever, seen in modern times. In order to address a critical need in the Mn neurotoxicity literature, we designed and implemented a cross-sectional exploratory neuropathological study of the corpus striatum in Mn and non-Mn mine workers in The Republic of South Africa, which contains over 80% of the world's Mn reserves.

This study is the largest neuropathology series of Mn exposed individuals, the first study to evaluate the neuropathology of

chronic low-level exposure, and the first quantitative histopathological/immunohistochemical study using a carefully matched reference group. Pathological characterization of the pre-clinical stage of chronic low-level exposure in human tissues is important for further disease characterization, biomarker discovery, and therapy development.

2. Methods

2.1. Sample acquisition

This study was approved by the Washington University Human Research Protection Organization (Saint Louis, MO, USA) and the University of the Witwatersrand Human Research Ethics Committee (Republic of South Africa; RSA). Under the Occupational Diseases in Mines and Works Act of the RSA, deceased mine workers have the right to a cardio-pulmonary autopsy, regardless of the cause of death, on condition that consent is provided by the next of kin (Myers et al., 1987). The families of deceased mine workers are eligible for financial compensation for specific mining-related pulmonary diseases. We built on this existing program by using a regionally based occupational health nurse to recruit potential brain donors from Mn and other mines. The Mn mines are located in a remote region of South Africa in the Northern Cape Province close to the Botswana border. There are several Mn mines located in close proximity to each other as the economically viable Mn field covers an area of approximately 35 km × 15 km (Gutzmer, 1996). The subjects in this study were employed by various mines in this region.

Upon notification of the death of a mine worker, the occupational health nurse consented and interviewed the next-of-kin. The brain specimens were suspended in 10% neutral buffered formalin for a minimum of three weeks, after which they were shipped to Washington University for ex vivo MRI imaging, and then to the University of Washington (Seattle, WA, USA) for pathological analysis. Investigators performing the cell density examinations, immunohistochemical stains, and cell density quantifications were blinded to exposure status.

2.2. Brain specimen processing and examination

At the University of Washington, a certified neuropathologist performed an external gross examination, including assessment of cerebral cortical atrophy. The cerebrum and posterior fossa contents were embedded in a 3% agar solution and sliced coronally and axially, at 4 mm intervals. A standard gross examination was undertaken, including an assessment of atrophy or discoloration of the corpus striatum and degree of pigmentation of the substantia nigra and locus caeruleus. Tissue sampling of several brain regions was performed, including but not limited to, bilateral cortices, hippocampi, basal ganglia, midbrain, pons, and cerebellum. These samples were processed for 24 h in an automated tissue processor and were subsequently embedded in paraffin wax to produce formalin-fixed paraffin embedded (FFPE) tissue blocks.

2.3. Immunohistochemistry

FFPE tissue blocks were sectioned with a microtome producing 4 μm thick tissue sections which were placed on positively-charged glass slides. Deparaffinized rehydrated slides were stained with hematoxylin and eosin (H&E) to examine morphology and to note any neurohistopathological changes. Utilizing previously optimized conditions, automated immunohistochemistry was performed on tissue sections from the basal ganglia, using a Leica Bond III Fully Automated IHC and ISH Staining System (Leica Bio-Systems, USA). Mouse monoclonal antibodies for glial fibrillary

acidic protein (GFAP) (Dako, USA) to label astrocytes, microtubule associated protein-2 (MAP-2) (Millipore USA) to label neurons, and CD68 (Dako, USA) to label macrophages and microglia, were diluted with the Leica Bond Primary Antibody Diluent (Leica Bio-Systems, USA) at 1:150, 1:1500, and 1:8000, respectively. For GFAP and MAP-2, an epitope retrieval step consisting of citrate buffer at 98 °C for 20 min (pH 5.9–6.1) was performed. For CD68, the epitope retrieval step consisted of 20 min EDTA-TRIS buffer (pH 8.9–9.1). The final step included the Bond Polymer Define Detection System (Leica Bio-Systems, USA), which includes endogenous peroxidase blocking, anti-mouse secondary antibody, and a streptavidin-biotin immunoenzymatic antigen detection system. The slides were then counterstained with Gill's hematoxylin. Appropriate positive and negative controls were included with each antibody run.

2.4. Cell density study

FFPE tissue blocks corresponding to a unilateral, coronal section of the corpus striatum were selected at the level of the interventricular foramen immediately posterior to the genu of the internal capsule on which both the globus pallidus external segment (GPe), and globus pallidus internal segment (GPi) were present, alongside the caudate and putamen. The regions of interest of the caudate, putamen, GPe, and GPi were delineated on the glass slides. Blinded observers were trained for each different cell type/antibody stain and taught the histological criteria, by a board certified neuropathologist. The training period also included supervised counting to assess for reproducibility and offer feedback about appropriate use of the histological criteria for each antibody. One observer counted the four regions only for GFAP and CD68 whereas the other observer counted the regions for MAP-2.

In each region, in addition to immunoreactivity, histological criteria were also utilized to classify different cell types, specifically: (1) astrocytes – cytoplasmic and GFAP immunoreactive processes and typical round nuclear morphology; (2) microglia – CD68 immunoreactive dot-like small thin processes and CD68-immuno negative nuclei along with cylindrical/amoeboid morphology; (3) neurons – cytoplasmic MAP-2 immunoreactivity as well as vesicular nuclei and/or nucleoli. CD68 antibody stains macrophages in addition to microglia. Therefore, when counting microglia, in addition to CD68 positivity, we also considered the morphology of the cells, i.e. microglia contain cytoplasmic processes characteristic of ramified or amoeboid microglia, whereas macrophages typically are foamy and with hemosiderin. To this end, these macrophages were rarely present.

For each subject, the four regions of interest (caudate, putamen, GPe, and GPi) were assessed with the aid of three different antibodies (GFAP-astrocytes, MAP-2-neurons, CD68-microglia). Using the aforementioned histological criteria, assessment consisted of counting the immunoreactive cells twice. Each "count" comprised 10 non-overlapping high power fields (HPF), totaling 20 non-overlapping HPFs per antibody per region per subject. HPF is defined as the field of view on a 40× objective [in this case performed with a BH45 light microscope (Olympus, Japan), corresponding to a field diameter of 550 µm]. From these counts, the average number of immunoreactive cells was calculated for one HPF per region for each subject. For one subject, fewer than 20 HPF were available; therefore, 10 HPF were counted on the slides for GFAP and CD68.

2.5. Exposure assessment

Upon notification of the death of a mine worker, and after obtaining consent from the next of kin for the removal of the brain

and cardio-respiratory organs, the occupational health nurse interviewed the family to obtain occupational and medical histories. During the consent process, permission to access the deceased mine worker's medical and employment records was also requested to verify the accuracy of the historical information. All mine workers undergo an annual employee medical examination. Medical charts were reviewed by the occupational health nurse. An industrial hygienist reviewed the occupational history and employment records and assigned a duration of Mn exposure in years (henceforth called "exposure years") to each subject when sufficient data were available. Although no Mn exposure data are available for these particular mine workers, measurements from two South African Mn mines, taken over a four-year period and averaged for particular mine jobs, ranged from 0.19 to 0.78 mg/m³ (Myers et al., 2003). The average intensity of exposure (cumulative exposure index/length of service in years) was 0.21 mg/m³ with an upper limit of 0.99 mg/m³. Earlier historical measurements are, unfortunately, not available. The Mn content of the rock in this area varies from 20 to 60% (Preston 2001). The use of duration of exposure in lieu of cumulative exposure is not unusual in occupational epidemiology, and has been demonstrated to be methodologically and statistically sound in certain instances. Thus, we believe that using duration of employment in the Mn mines is an acceptable surrogate for exposure in this study.

2.6. Statistical analysis

Since this was an exploratory study, we did not correct for multiple comparisons, in order to ensure that we identified any trend in cell density differences to guide future studies. We compared mean cell counts per HPF in Mn and non-Mn mine workers, using a two tailed *t*-test. Spearman's correlations were performed to compare exposure years and cell counts. Dichotomous variables were compared using chi-square tests. Statistical significance was set at 5%.

3. Results

Using the recruitment methods described above, we received brains from 28 male mine workers. All 28 brains underwent a general gross examination by a board certified neuropathologist, and those with evidence of significant maceration or putrefaction were excluded from the analysis (*n* = 12). The remaining 16 brains were histologically assessed to evaluate architectural integrity. Eight Mn mine workers and eight age-matched non-Mn mine worker reference subjects, with brain tissue of suitable quality to perform neuropathological and immunohistochemical examinations were included in the study. The demographic characteristics of the mine workers, and their work histories, causes of death and disease status are shown in Tables 1 and 2. Review of the medical records indicated that none of the subjects had parkinsonian symptoms or any other neurological conditions. Gross neuropathological examinations did not reveal any evidence of pathologically relevant cortical or striatal atrophy, pallidal discoloration, depigmentation of the substantia nigra and/or locus coeruleus.

Table 1

Demographic characteristics of Mn and non-Mn mine workers.

	Mn mine workers (<i>n</i> = 6)			Non-Mn mine workers (<i>n</i> = 8)		
	Mean	Min	Max	Mean	Min	Max
Age at death	57.28	46.43	70.59	60.13	44.21	79.53
Years in Mn mines	11.91	1.20	31.41	0.00	0.00	0.00
Post-mortem interval (days)	5.13	2.00	9.00	4.63	2.00	9.00

Table 2

Work histories, causes of death, and disease status of Mn and non-Mn mine workers.

Commodity mined	Occupation	Years worked	Total years worked	Age at death	Clinical cause of death ^a	Other findings (including autopsy findings)
Mn mine workers						
1 Asbestos	Laborer	1964, 1973, 1976	1.6	67	Natural causes	Asbestosis
Diamond	Laborer	1965–1968, 1977–1984	11.0			
Manganese	Laborer, store minder	1974, 1985	2.0			
2 Manganese	Driver	1978–2009	31.4	57	Natural causes	Kidney failure, asbestosis, non-Hodgkin's lymphoma
3 Diamond	Miner	1978–2007	30.0	53	Natural causes	
Manganese	Miner	2008–2010	1.2			
4 Gold	Rigger	1961–1962	1.0	65	Natural causes	Asbestosis, hydatid cyst, aspergillosis
Platinum	Machine operator	1971–1978	7.0			
Manganese	Machine operator	1979–1980, 1982–1988	8.0			
Asbestos	Machine operator	1980, 1989–1992	4.4			
5 Asbestos	Sampler	1980	0.2	50	Natural causes	Broncho-pneumonia
Manganese	Machine operator	1995, 2003–2005	2.9			
6 Asbestos	Winch driver	1991–1992	1.8	46	Hemo-pericardium	Tuberculous pericarditis, focal PTB, tuberculous nodes
Manganese	Belt cleaner/attendant	2002–2009	7.7			
Asbestos	Jack hammer operator	Unknown	Unknown	70	Respiratory tract infection	Asthma, asbestosis, asbestos plaques
Manganese	Jack hammer operator	Unknown	Unknown			
Manganese	Locomotive operator	1988–2001	22.8	45	Natural causes	PTB, tuberculous pericarditis
Non-Mn mine workers						
1 Asbestos	Miner's assistant	1952–1953, 1956–1957, 1972	2.3	79	Asthma, emphysema	Asthma, emphysema, diabetes, PTB
Coal	Laborer	Unknown	Unknown			
2 Asbestos	Laborer	1981–1987	6.0	45	PTB	PTB
Platinum	Various	1992–2004	12.0			
Iron ore	Laborer	2007–2008	0.7			
3 Asbestos	Unknown	1987–1992	Unknown	48	Natural causes	PTB, asbestos plaques, pneumocystis pneumonia
4 Diamond	Laborer	1961–1968	6.0			
Asbestos	Stamper	1969	0.6			
5 Asbestos	Various	1977–1978, unknown	Unknown	53	Natural causes	PTB
6 Gold	Various	1991–1996	5.5	44	Natural causes	PTB, silicosis
7 Diamond	Miner	1967–1970	3.5	62	Natural causes	Diabetes, asthma, hypertension, asbestosis
8 Asbestos	Welder/laborer	1971–1974	3.5			
Asbestos	Various	1976–1992	15.8	74	Natural causes	Hypertension, military tuberculosis, pleural plaques
Gold	Miner's assistant	2010–2012	2.3			

PTB, pulmonary tuberculosis.

^a As written on the death certificate, or from details provided on documentation submitted with organs.

Conventional histologically stained sections of the regions of interest as well as those from the frontal cortex, temporal cortex, hippocampus, and cerebellum did not reveal any definite evidence of HIV encephalitis (including perivascular multinucleated giant cells or microglial nodules), stroke, demyelination, or a neoplastic process. Two subjects in the non-Mn mine worker reference group had lacunar infarctions that were not present on the side and/or at the level of the tissue sections studied.

Mn mine workers had lower mean astrocyte densities in the caudate and putamen [9.85 (SD 3.94) and 8.91 (SD 3.64) cells per HPF, respectively] than non-Mn mine workers [12.86 (SD 3.90), and 11.63 (SD 2.97) cells per HPF in the caudate and putamen, respectively] (caudate $p = 0.146$, putamen $p = 0.125$). Although the differences were not statistically significant, this represents a 19% lower astrocyte density in Mn mine workers, in both the caudate and putamen. The external and internal segments of the globus pallidus in the Mn and non-Mn mine workers had very similar astrocyte densities. Mn mine workers also had lower mean neuron densities in the caudate and putamen [16.50 (SD 6.79) and 16.00 (SD 7.16) cells per HPF] than non-Mn mine workers [19.90 (SD 3.72) and 18.10 (SD 3.30) cells per HPF in the caudate and putamen, respectively] (caudate $p = 0.235$, putamen $p = 0.455$) (Fig. 1b). This represents a 14% and 8% lower neuron density in the caudate and putamen of Mn mine workers, respectively. Neuronal

density in the GPi was higher in the Mn than non-Mn mine workers [2.05 (SD 0.81) and 1.28 (SD 0.39) cells per HPF, respectively; $p = 0.028$].

In contrast to neuronal and astroglial counts, Mn mine workers had higher microglial densities in both the external and internal segments of the globus pallidus than the non-Mn mine workers [1.33 (SD 0.55) and 1.37 (SD 0.75) cells per HPF, respectively for Mn mine workers, and 0.87 (SD 0.34) and 0.99 (SD 0.49) cells per HPF respectively for non-Mn exposed mine workers]. These represent 52% and 38% higher microglial densities in the external and internal segments of the globus pallidus of Mn mine workers, respectively.

In all examined brain regions, the Mn mine workers had lower ratios of astrocytes to microglia compared to the non-Mn mine workers. The astrocyte to microglia ratio was significantly lower in the caudate in the Mn mine workers (7.80; SD 2.27) compared to the non-Mn mine workers (14.68 (SD 6.81), respectively, $p = 0.025$). The other regions trended toward lower astrocyte to microglia ratios; GPe (10.60; SD 4.10 and 16.10; SD 7.51, respectively), putamen (7.35; SD 2.63 and 11.11; SD 5.81, respectively), and the GPi (9.56; SD 5.88 and 12.42; SD 6.64, respectively); however, these were not statistically significant.

We also investigated the association between cumulative years worked and cell density in the caudate nucleus, putamen, and

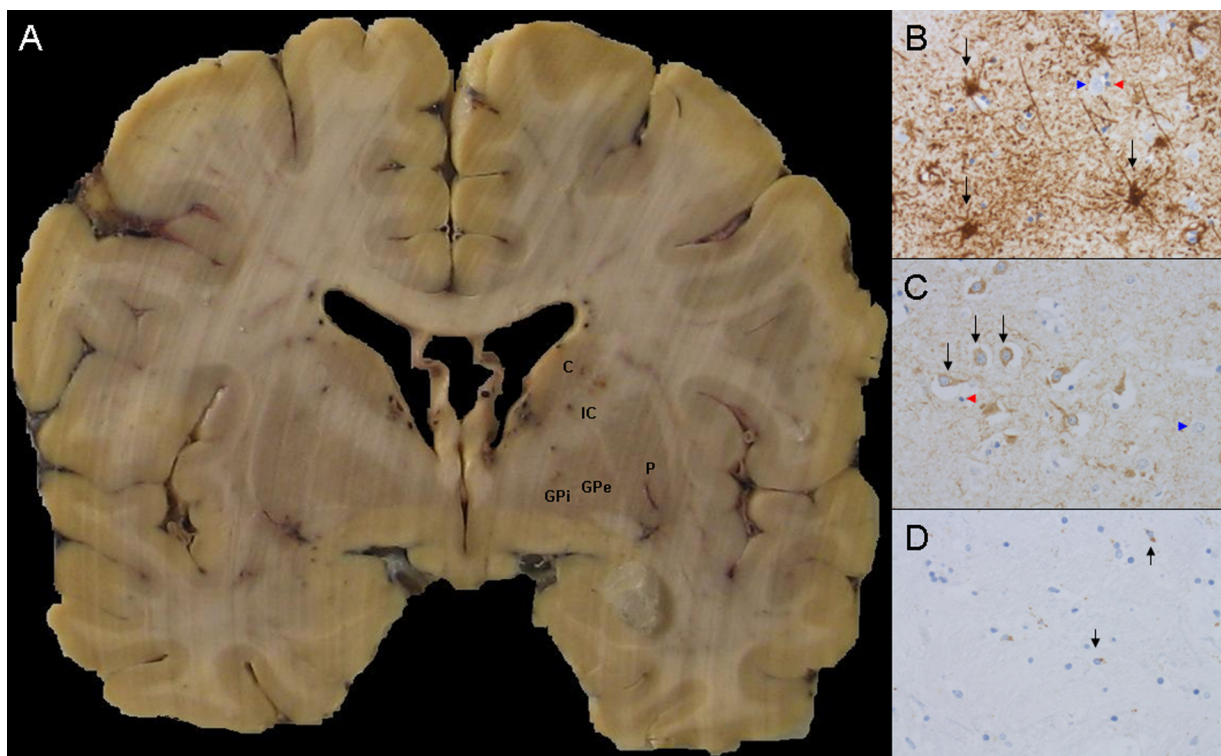


Fig. 1. Gross and immunohistochemical sections. (A) Representative coronal section demonstrating the basal ganglia level where histological sampling was undertaken (C – caudate, P – putamen, IC – internal capsule, GPe – globus pallidus externa, GPi – globus pallidus interna). (B) Representative high power ($40\times$) GFAP-stained sections from an Mn exposed subject (black arrows demonstrate representative immunoreactive astrocytes, blue arrowheads show non-immunoreactive neurons, red arrowheads show non-immunoreactive oligodendrocytes). (C) Representative high power ($40\times$) MAP2-stained sections from an Mn exposed subject, (black arrows demonstrate representative immunoreactive neurons, blue arrowheads show non-immunoreactive astrocytes, red arrowheads show non-immunoreactive oligodendrocytes). (D) Representative high power ($40\times$) CD68-stained sections from an Mn exposed subject (black arrows demonstrate representative immunoreactive microglia).

internal and external segments of the globus pallidus in the Mn mine workers (Table 3). Among the mine workers with detailed work histories ($n = 6$), there was a significant correlation between microglial density in the GPi and years worked (Spearman's rho = 0.886; $p = 0.019$; Table 4). There was no correlation between age and years worked in the Mn mines. (Spearman's rho = 0.371; $p = 0.468$), suggesting that the correlation between microglial density in the GPi and exposure was not confounded by age (Table 5).

4. Discussion

Previously, we demonstrated the feasibility of undertaking this novel occupational neuropathology program (Nelson et al., 2012).

The recruitment of a large number of deceased mine workers whose families were willing to donate their brains for neuropathological examination facilitated a carefully matched exposed/non-exposed comparison study. Previous neuropathological studies found neuronal loss and gliosis in subjects with symptomatic manganism, but these were mostly qualitative reports without controls, so the neuropathological "hallmarks" of symptomatic manganism remain speculative (Ashizawa, 1927; Canavan et al., 1934; Stadler, 1936; Trendtel, 1936; Parnitzke, 1954). There are several important findings in this study. Quantitative histopathological cell density demonstrated a trend toward lower astrocyte and neuron density in the caudate and putamen as well as higher microglial density in the globus pallidus of Mn mine workers without neurological diagnoses, compared to non-Mn mine workers, although the trend was not statistically significant. Moreover, the ratios of astrocytes to microglia were lower in all brain regions assessed in Mn mine workers compared to non-Mn mine workers, suggesting that the pre-clinical stage of Mn induced neurotoxicity might be characterized by an inflammatory response

Table 3
Cell density in corpus striatum.

Stained region per high power field (HPF)	Mn mine workers ($n=8$)	Non-Mn mine workers ($n=8$)	% Difference	<i>p</i> value
Astrocytes caudate	9.85 ± 3.94	12.86 ± 3.90	23% ↓	0.146
Astrocytes putamen	8.91 ± 3.64	11.63 ± 2.97	23% ↓	0.125
Astrocytes GPe	12.80 ± 3.68	12.40 ± 3.64		0.846
Astrocytes GPi	10.60 ± 2.66	10.60 ± 3.64		0.979
Microglia caudate	1.25 ± 0.30	1.18 ± 1.01		0.856
Microglia putamen	1.29 ± 0.50	1.24 ± 0.60		0.859
Microglia GPe	1.33 ± 0.55	0.87 ± 0.34	53% ↑	0.064
Microglia GPi	1.37 ± 0.75	0.99 ± 0.49	38% ↑	0.250
Neurons caudate	16.50 ± 6.79	19.90 ± 3.72	17% ↓	0.235
Neurons putamen	16.00 ± 7.16	18.10 ± 3.30	11% ↓	0.455
Neurons GPe	1.87 ± 0.86	1.34 ± 0.52	40% ↑	0.162
Neurons GPi	$2.05 \pm 0.81^*$	1.28 ± 0.39	60% ↑	0.028^

GPe, globus pallidus external segment; GPi, globus pallidus internal segment.

* $p < 0.05$, two tailed *t*-test.

Table 4
Ratio of astrocytes to microglia in corpus striatum.

	Mn mine workers	Non-Mn exposed mine workers	<i>p</i> value
GFAP/CD68 ratio caudate	7.80 ± 2.27	14.68 ± 6.81	0.025^
GFAP/CD68 ratio putamen	7.35 ± 2.63	11.11 ± 5.81	0.117
GFAP/CD68 ratio GPe	10.60 ± 4.10	16.10 ± 7.51	0.091
GFAP/CD68 ratio GPi	9.56 ± 5.88	12.42 ± 6.64	0.376

GPe, globus pallidus external segment; GPi, globus pallidus internal segment.

* $p < 0.05$.

Table 5

Correlation between cell density and exposure years.

Stained region per high power field (HPF)	Average years worked in Mn mines (n=6)	
	Spearman's rho	p value
Astrocytes caudate	0.314	0.544
Astrocytes putamen	0.429	0.397
Astrocytes GPe	0.429	0.397
Astrocytes GPi	0.143	0.787
Microglia caudate	0.543	0.266
Microglia putamen	0.600	0.208
Microglia GPe	0.406	0.425
Microglia GPi	0.886	0.019*
Neurons caudate	0.371	0.468
Neurons putamen	0.771	0.072
Neurons GPe	0.429	0.397
Neurons GPi	-0.371	0.468

GPe, globus pallidus external segment; GPi, globus pallidus internal segment.

* $p < 0.05$.

to Mn deposition, followed by striatal injury to astrocytes which, in turn, may lead to disturbed homeostasis of the neuropil and to neuronal injury. This is consistent with the hypothesized mechanism behind restricted diffusion found in the striatum of Mn exposed welders on diffusion weighted MRI (Criswell et al., 2012). A larger study using more precise cell counting methods is needed to confirm these findings.

While a larger sample size is needed to confirm these findings, we believe that the current study provides a unique perspective on the early pathological associations with Mn exposure. Increased signal in the globus pallidus on T1 MRI with normal signal on T2 is pathognomonic of Mn over-exposure (Criswell et al., 2012; Nelson et al., 1993). The finding of greater microglial density in Mn exposed versus non-exposed subjects, and correlation with years of exposure suggests that Mn deposition induces a microglial response and that this signal may be due, in part, to an inflammatory response to tissue Mn deposition. Interestingly, we have previously shown that this signal can remain years after removal from the source of exposure, (Nelson et al., 2012) and microglial infiltration may underlie this signal change. Astrocytes express high affinity metal transporters capable of Mn transport, such as the divalent metal transporter (DMT1), allowing astrocytes to accumulate as much as 50-fold higher Mn concentrations than neurons (Filipov and Dodd, 2012; Hazell, 2002; Aschner et al., 1992). Once inside astrocytes, Mn accumulates in the mitochondria where it inhibits oxidative phosphorylation, leading to increased reactive oxygen species production; it also promotes the secretion of various inflammatory mediators (Filipov and Dodd, 2012; Aschner et al., 1992; Gavin et al., 1990). Neuronal toxicity associated with Mn exposure may be due to impaired astrocytic glycine uptake, leading to neurotransmitter dysregulation (Sidoryk-Wegrzynowicz et al., 2009; Milatovic et al., 2007).

Interestingly, the trends toward lower astrocyte and neuronal density in the striatum are probably occurring in the setting of exposures that are less than the Occupational Safety and Health Administration (OSHA) ceiling for inhaled Mn of 5 mg/m (Myers et al., 2003). In fact, most mine workers in Myers et al.'s study, conducted in the same Mn mine region from which we obtained our neuropathological specimens, had exposures that were lower than the American Conference of Governmental Industrial Hygienists (ACGIH) permissible exposure limit of 0.2 mg/m (Myers et al., 2003). While we do not have exposure data for these mine workers, further study of Mn exposed mine workers in these mines, using highly sensitive pathological health outcome data, may permit exposure-pathology correlations that could redefine the allowable exposure thresholds. There is considerable evidence

supporting cognitive, mood, and motor toxicity at Mn exposure levels within the OSHA and ACGIH exposure limits (Bowler et al., 1999, 2011; Lucchini et al., 1999). Clinical pathological correlations will be necessary to understand the pathophysiology of the clinical neurotoxicity and to determine if Mn neurotoxicity is associated with degenerative pathologies.

Recent data obtained from Mn exposed welders, using PET imaging with 6-[¹⁸F] fluoro-L-DOPA (FDOPA), suggest that chronic exposure to Mn containing welding fume is associated with striatal pre-synaptic dopaminergic dysfunction (Criswell et al., 2011). Interestingly, we found that the mean neuronal counts in Mn mine workers were 8% and 14% lower than in non-Mn mine workers in the caudate and putamen, respectively. The magnitude of the observed difference is consistent with the 10% reduction pre-synaptic dopaminergic function found in our welder study (Criswell et al., 2012). While the current study focused on the corpus striatum, the lower astrocyte counts may indicate that the pre-synaptic dopaminergic dysfunction found in Mn exposed welders may be secondary to terminal field neurotoxicity, possibly mediated through a loss of astrocytes. In fact, there is growing evidence that the sites of primary neuronal injury in degenerative basal ganglia disorders such as Parkinson disease are mediated through "dying back phenomena" (Choi et al., 2011; Galvin et al., 1999).

As with any cross-sectional autopsy study, this study had notable limitations. First, the sample size was relatively small compared to large Parkinson and Alzheimer disease pathological series. However, the eight subjects reported here represent the largest group of Mn mine workers ever studied histopathologically. Our exploratory study demonstrates feasibility of obtaining diagnostically viable tissue from this remote region of South Africa, and indicates that it is possible to conduct a large, definitive neuropathological study of chronic Mn exposure. A larger sample of Mn mine workers with more precise lifetime exposure reconstruction across a broader range of exposures will be needed to explore exposure-pathology relationships, especially with neurons and astrocytes. Similarly, the health outcome data available in this study were limited to information obtained at routine medical office visits and annual employee occupational health examinations. Efforts to improve the quantity and quality of the health outcome data in living Mn mine workers is ongoing, which will benefit future studies. Second, the finding of higher neuronal density in the globus pallidus is biologically uninterpretable and of unclear significance. Given that, in adult primates, neurons are terminally differentiated and thought not to divide, the findings of our study may be compromised by the limited sample size. While cell density studies may not be as precise as stereological counting, HPFs are units routinely used by pathologists and provide useful information in the clinical setting. The associations suggested in this study need to be confirmed, using a larger sample and more precise counting methods, using stereology techniques to reduce type II error. Nevertheless, this study provides critical data to inform future Mn neuropathology studies.

5. Conclusion

In summary, this exploratory occupational neuropathology study of the pre-clinical stage of chronic low-level Mn exposure demonstrates a trend toward lower astrocyte and neuron densities in the striatum and an inflammatory microglial response in the globus pallidus. Recruitment from this population has proven feasible and the tissue quality is suitable for pathologic analysis. We anticipate future studies using non-biased stereology to investigate the trends described above in Mn and non-Mn miner reference subjects. In addition, acquiring neuropathology from workers in whom we have detailed clinical examinations will permit clinical-pathologic correlation. Finally, ex vivo MRI imaging will be used to correlate tissue metal concentrations

and pathology to identify imaging biomarkers of Mn exposure and neurotoxicity.

Conflicts of interest statement

The authors declare that there are no conflicts of interest.

Grant support

The authors of this study were supported by the following entities:

LFGC: National Institute for Environmental Health Sciences (NIEHS) (R01ES019277-02S1). GN: NIEHS (R21ES17504, the St. Louis Chapter of the American Parkinson Disease Association. SC: NIH [K23 ES021444-01]. HC: NIEHS, National MS society. BAE: NIH Grant UL1 RR024992. JM: NIEHS (R21ES17504, the St. Louis Chapter of the American Parkinson Disease Association. JZ: NIEHS (R01ES019277). BAR: NIEHS (R21ES17504, K24 ES017765, P42ES004696), the Michael J. Fox Foundation, NINDS Grant Number 5T32NS007205-27, NCRRO and NIH Roadmap for Medical Research Grant Number UL1 RR024992 and UL1 TR000448, the St. Louis Chapter of the American Parkinson Disease Association.

The study sponsors had no involvement in study design; collection, analysis, and interpretation of data; the writing of the manuscript; or the decision to submit the article for publication.

Acknowledgements

We like to thank Sr. Marina Steenkamp and Dr. Johan Mostert for tissue acquisition, and Julian Mthombeni for laboratory assistance in South Africa. In addition, we would like to thank Dr. C. Dirk Keene, Dr. Thomas Montine, and Dr. Joshua Sonnen as well as Ms. Kim Howard and Ms. Aimee Schantz from the University of Washington for input and support during specimen processing. In addition we appreciate the work from Ms. Toni Baulinger, Ms. Regina Bowman, Mr. J. Matthew Brooks, and Ms. Susan Rozell from the University of Washington Neurohistology department for H&E stains, tissue processing, and immunohistochemical staining and optimization.

References

Aschner M, Gannon M, Kimelberg HK. Manganese uptake and efflux in cultured rat astrocytes. *Journal of Neurochemistry* 1992;58(2):730–5.

Ashizawa R. Über einen sektionsfall von chronischer. *Japanese Journal of Science Transactions of Internal Medicine Pediatrics and Psychiatry* 1927;1:173–91.

Bernheimer H, Birkmayer W, Hornykiewicz O, Jellinger K, Seitelberger F. Brain dopamine and the syndromes of Parkinson and Huntington. Clinical, morphological and neurochemical correlations. *Journal of the Neurological Sciences* 1973;20(4):415–55.

Bowler RM, Mergler D, Sassine MP, Larribe F, Hudnell K. Neuropsychiatric effects of manganese on mood. *Neurotoxicology* 1999;20(2–3):367–78.

Bowler RM, Gocheva V, Harris M, Ngo L, Abdelouhab N, Wilkinson J, et al. Prospective study on neurotoxic effects in manganese-exposed bridge construction welders. *Neurotoxicology* 2011;32(5):596–605.

Bowman AB, Kwakye GF, Hernandez EH, Aschner M. Role of manganese in neurodegenerative diseases. *Journal of Trace Elements in Medicine and Biology* 2011;25(4):191–203.

Canavan M, Cobb S, CK D. Chronic manganese poisoning. *Archives of Neurology and Psychiatry* 1934;32(3):501–12.

Casamajor L. An unusual form of mineral poisoning affecting the nervous system: manganese. *Journal of the American Medical Association* 1913;60(9):646–9.

Choi WS, Palmerit RD, Xia Z. Loss of mitochondrial complex I activity potentiates dopamine neuron death induced by microtubule dysfunction in a Parkinson's disease model. *Journal of Cell Biology* 2011;192(5):873–82.

Cooper WC. The health implications of increased manganese in the environment resulting from the combustion of fuel additives: a review of the literature. *Journal of Toxicology and Environmental Health* 1984;14(1):23–46.

Couper J. On the effects of black oxide manganese when inhaled in the lungs. *British Annals of Medicine and Pharmacology* 1837;1:41–2.

Criswell SR, Perlmuter JS, Videen TO, Moerlein SM, Flores HP, Birke AM, et al. Reduced uptake of [(1)F]FDOPA PET in asymptomatic welders with occupational manganese exposure. *Neurology* 2011;76(15):1296–301.

Criswell SR, Perlmuter JS, Huang JL, Golchin N, Flores HP, Hobson A, et al. Basal ganglia intensity indices and diffusion weighted imaging in manganese-exposed welders. *Occupational and Environmental Medicine* 2012;69(6):437–43.

Filipov NM, Dodd CA. Role of glial cells in manganese neurotoxicity. *Journal of Applied Toxicology* 2012;32(5):310–7.

Flynn MR, Susi P. Manganese, iron, and total particulate exposures to welders. *Journal of Occupational and Environmental Hygiene* 2010;7(2):115–26.

Galvin JE, Uryu K, Lee VM, Trojanowski JQ. Axon pathology in Parkinson's disease and Lewy body dementia hippocampus contains alpha-, beta-, and gamma-synuclein. *Proceedings of the National Academy of Sciences of the United States of America* 1999;96(23):13450–5.

Gavin CE, Gunter KK, Gunter TE. Manganese and calcium efflux kinetics in brain mitochondria. Relevance to manganese toxicity. *Biochemical Journal* 1990;266(2):329–34.

Gutzmer J. Genesis and alteration of the Kalahari and Postmasburg manganese deposits, Griqualand West, South Africa. 1996.

Hazell AS. Astrocytes and manganese neurotoxicity. *Neurochemistry International* 2002;41(4):271–7.

Hobson A, Seixas N, Sterling D, Racette BA. Estimation of particulate mass and manganese exposure levels among welders. *Annals of Occupational Hygiene* 2011;55(1):113–25.

Liu S, Hammond SK, Rappaport SM. Statistical modeling to determine sources of variability in exposures to welding fumes. *Annals of Occupational Hygiene* 2011;55(3):305–18.

Lucchini R, Apostoli P, Perrone C, Placidi D, Albini E, Migliorati P, et al. Long-term exposure to low levels of manganese oxides and neurofunctional changes in ferroalloy workers. *Neurotoxicology* 1999;20(2–3):287–97.

Milatovic D, Yin Z, Gupta RC, Sidoryk M, Albrecht J, Aschner JL, et al. Manganese induces oxidative impairment in cultured rat astrocytes. *Toxicological Sciences: An Official Journal of the Society of Toxicology* 2007;98(1):198–205.

Milatovic D, Zaja-Milatovic S, Gupta RC, Yu Y, Aschner M. Oxidative damage and neurodegeneration in manganese-induced neurotoxicity. *Toxicology and Applied Pharmacology* 2009;240(2):219–25.

Myers JE, Garisch D, Cornell JE. Compensation for occupational diseases in the RSA. *South African Medical Journal* 1987;71(5):302–6.

Myers JE, teWaterNaude J, Fourie M, Zogoe HB, Naik I, Theodorou P, et al. Nervous system effects of occupational manganese exposure on South African manganese miners. *Neurotoxicology* 2003;24(4–5):649–56.

Nelson K, Golnick J, Korn T, Angle C. Manganese encephalopathy: utility of early magnetic resonance imaging. *British Journal of Industrial Medicine* 1993;50(6):510–3.

Nelson G, Criswell SR, Zhang J, Murray J, Racette BA. Research capacity development in South African manganese mines to bridge exposure and neuropathologic outcomes. *Neurotoxicology* 2012;33(4):683–6.

Parnitzke KP. Zur klinik und pathologischen anatomie der chronischen braunsteinvergiftung. *Archiv für Psychiatrie und Zeitschrift Neurologie* 1954;192:405–19.

Racette BA, Tabbal SD, Jennings D, Good L, Perlmuter JS, Evanoff B. Prevalence of parkinsonism and relationship to exposure in a large sample of Alabama welders. *Neurology* 2005;64(2):230–5.

Racette BA, Criswell SR, Lundin JI, Hobson A, Seixas N, Kotzbauer PT, et al. Increased risk of parkinsonism associated with welding exposure. *Neurotoxicology* 2012;33(5):1356–61.

Rodier J. Manganese poisoning in Moroccan miners. *British Journal of Industrial Medicine* 1955;12(1):21–35.

Sidoryk-Wegrzynowicz M, Lee E, Albrecht J, Aschner M. Manganese disrupts astrocyte glutamine transporter expression and function. *Journal of Neurochemistry* 2009;110(3):822–30.

Stadler H. Zur histopathologie des gehims bei manganvergiftung. *Zeitschrift für die gesamte Neurologie und Psychiatrie* 1936;154:62–76.

Teeguarden RG, Dorman DC, Covington TR, Clewell HJ 3rd, Andersen ME. Pharmacokinetic modeling of manganese. I. Dose dependencies of uptake and elimination. *Journal of Toxicology and Environmental Health Part A* 2007;70(18):1493–504.

Teeguarden RG, Dorman DC, Nong A, Covington TR, Clewell HJ 3rd, Andersen ME. Pharmacokinetic modeling of manganese. II. Hepatic processing after ingestion and inhalation. *Journal of Toxicology and Environmental Health Part A* 2007;70(18):1505–14.

Trendtel F. Zur Frage des Manganismus. *Mschr Unfallheilk* 1936;43:69–84.

Wang JD, Huang CC, Hwang YH, Chiang JR, Lin JM, Chen JS. Manganese induced parkinsonism: an outbreak due to an unrepairs ventilation control system in a ferromanganese smelter. *British Journal of Industrial Medicine* 1989;46(12):856–9.

Yamada M, Ohno S, Okayasu I, Okeda R, Hatakeyama S, Watanabe H, et al. Chronic manganese poisoning: a neuropathological study with determination of manganese distribution in the brain. *Acta Neuropathologica* 1986;70(3–4):273–8.